

Lévy walk dynamics in an external harmonic potential

Pengbo Xu,¹ Tian Zhou,¹ Ralf Metzler,² and Weihua Deng¹

¹*School of Mathematics and Statistics, Gansu Key Laboratory of Applied Mathematics and Complex Systems, Lanzhou University, Lanzhou 730000, P.R. China*

²*Institute for Physics & Astronomy, University of Potsdam, Karl-Liebknecht-St 24/25, 14476 Potsdam, Germany*

Lévy walks (LWs) are spatiotemporally coupled random-walk processes describing superdiffusive heat conduction in solids, propagation of light in disordered optical materials, motion of molecular motors in living cells, or motion of animals, humans, robots, and viruses. We here investigate a key feature of LWs, their response to an external harmonic potential. In this generic setting for confined motion we demonstrate that LWs equilibrate exponentially and may assume a bimodal stationary distribution. We also show that the stationary distribution has a horizontal slope next to a reflecting boundary placed at the origin, in contrast to correlated superdiffusive processes. Our results generalize LWs to confining forces and settle some long-standing puzzles around LWs.

PACS numbers: 02.50.-r, 05.30.Pr, 02.50.Ng, 05.40.-a, 05.10.Gg

Anomalous diffusion with mean squared displacement (MSD) $\langle x^2(t) \rangle \simeq t^\alpha$, whose anomalous diffusion exponent differs from the value $\alpha = 1$ of Brownian motion, are ubiquitously observed in a wide range of systems [1–3]. Subdiffusion with $0 < \alpha < 1$ occurs in amorphous semiconductors [4], artificially crowded liquids [5], lipid bilayer membranes [6–8], cytoplasm of biological cells [9, 10], or in hydrology [11]. Superdiffusion with $\alpha > 1$ is observed in active systems such as molecular motor transport in cells [12–14] or in turbulence [15]. One of the central stochastic models for both regimes of anomalous diffusion is the continuous time random walk (CTRW), based on the two identically distributed random variables of the waiting times τ in between any two jumps and the single jump lengths x [1, 4, 16, 17]. In the hydrodynamic limit uncoupled CTRW processes in an external potential can be conveniently described in terms of time- and/or space-fractional Fokker-Planck equations [17–20].

Superdiffusion is often modeled by Lévy flights (LFs), CTRWs with exponential waiting time probability density function (PDF) and power-law jump length PDF $\lambda(x) \simeq |x|^{-1-\mu}$ ($0 < \mu < 2$) [19]. The scale-free nature of $\lambda(x)$ translates into a diverging MSD, but transport can be characterized in terms of fractional order moments $\langle |x|^\kappa \rangle^{2/\kappa} \simeq t^{2/\mu}$ [17]. Due to their fractal, clustering motion pattern LFs are often used as efficient random search mechanisms, e.g., for foraging animals [21, 22]. In harmonic external potentials LFs have a stationary state yet diverging MSD [20]. In steeper than harmonic potentials LFs assume multimodal stationary PDFs with finite MSD but diverging higher-order moments [23].

A physically more pleasing CTRW concept for superdiffusion are Lévy walks (LWs), based on a spatiotemporal coupling of jump lengths and waiting times with a finite propagation speed and finite MSD [24, 25]. This property makes them ideal candidates for the description of anomalous heat transport [26], transport in Lorentz-like gases [27], and light propagation in disordered optical media [28]. LWs were shown to be efficient search strategies [29, 30], consistent with their first-hitting time prop-

erties [31], and may emerge from deterministic nonlinear systems near a critical point [32]. Indeed, LWs are observed in molecular-motor motion [33], spreading of cancer cells [34], human hunter-gatherer foraging [35], pedestrian movement [36], and in optimized robotic search [37]. LWs underly human movement patterns [38] and were identified in the COVID-19 pandemic propagation [39].

LWs are “ultra-weakly” non-ergodic and fulfill generalized fluctuation-dissipation relations [40, 41] and are related to infinite densities [42]. For constant external drift LWs are described by a fractional material derivative [43], for arbitrary external potentials LWs follow a generalized Kramers-Fokker-Planck equations [44]. The latter is hard to solve for concrete problems, as the Fourier-Laplace technique cannot be applied due to the spatiotemporal coupling. Here we report an explicit solution of LWs in a physically important harmonic potential. Answering some puzzles in LW theory, we demonstrate that the PDF relaxes *exponentially* to a *stationary limit* with a plateau value of the MSD that is independent of the exact formulation of the LW. We moreover demonstrate that the stationary PDF is *bimodal* in a wide parameter range. When the process approaches a regular random walk a monomodal stationary PDF is restored. The PDF is also shown to have a horizontal asymptote in the presence of a reflecting boundary placed at the origin.

The scenario with harmonic confinement is relevant for molecular motors tethered to a center (e.g., an intersection between microtubules in a cell, or a cargo that is stuck in the cytoskeleton) by a flexible linker. Similarly the LW could be a motor attached to a cargo that is in the harmonic potential of an optical tweezer. On a macroscopic scale, the harmonic confinement models the restriction on animal and human motion imposed by the “territory” (home range, quarantine restrictions, etc.).

LWs in harmonic external potential. We first consider a random walker with mass M and position x_t at time t in the harmonic potential $V(x_t) = \frac{\gamma}{2}x_t^2$ with constant $\gamma > 0$. Let x_t be the final position of each step of the LW. According to [25] we consider the starting velocity of each

step to be $\pm v_0$ ($v_0 > 0$) with probability of 1/2 for left and right ($-$ or $+$). This picture is similar to a skater, whose initial push is always identical. As the skater's speed diminishes while gliding, in the course of a step the LW's velocity is changed by the potential. Denote t_i ($i = 1, 2, \dots, n$) the time when the i th renewal event just finishes and assume that the duration $\tau = t_i - t_{i-1}$ between two renewal events obeys the density $\phi(\tau)$. Then

$$M d^2 x_{t_i+\tau'} / d\tau'^2 = -\gamma x_{t_i+\tau'}, \quad (1)$$

governs the dynamics between the i th and $(i+1)$ th renewals, for $t_i \leq t$ and $\tau' \in (0, \{t_{i+1} \wedge t\} - t_i]$, for initial position x_{t_i} and velocity $dx_{t_i+\tau'} / d\tau'|_{\tau'=0} = \pm v_0$. The solution of (1) is $x_{t_i+\tau'} = x_{t_i} \cos(\omega\tau') \pm \frac{v_0}{\omega} \sin(\omega\tau')$, where $\omega = \sqrt{\gamma/M}$. According to the theory of LWs [25],

$$q(x_{t'}, t') = \int_{-\infty}^{\infty} dx_{t'-\tau} \int_0^t q(x_{t'-\tau}, t' - \tau) \times v(x_{t'-\tau}, x_{t'}, \tau) \phi(\tau) dt_\tau + p_0(x_{t'}) \delta(t') \quad (2)$$

determines the PDF $q(x_{t'}, t')$ that the renewal event finishes at time $t' < t$ and the particle arrives at position $x_{t'}$. $p_0(x) = \delta(x)$ is the initial PDF and $v(x, y, \tau) = \frac{1}{2} \delta(y - x \cos(\omega\tau) + \frac{v_0}{\omega} \sin(\omega\tau)) + \frac{1}{2} \delta(y - x \cos(\omega\tau) - \frac{v_0}{\omega} \sin(\omega\tau))$. With the property of the delta function we rewrite (2) as

$$q(x_{t'}, t') - p_0(x) \delta(t') = (1/2) \int_0^{t'} \phi(\tau) d\tau / |\cos(\omega\tau)| \times [q(x_{t'}^+, t' - \tau) + q(x_{t'}^-, t' - \tau)], \quad (3)$$

where $x_{t'}^\pm = (x_{t'} / \cos(\omega\tau)) \pm (v_0/\omega) \tan(\omega\tau)$. The PDF $p(x, t)$ to find the particle at x at time t then satisfies

$$p(x, t) = \int_{-\infty}^{\infty} \int_0^t q(x_{t-\tau}, t-\tau) v(x_{t-\tau}, x, \tau) \Psi(\tau) d\tau dx_{t-\tau}, \quad (4)$$

where $\Psi(\tau) = \int_\tau^\infty \phi(\tau') d\tau'$. With $v(x_{t-\tau}, x, \tau)$ we get

$$p(x, t) = \frac{1}{2} \int_0^t \frac{\Psi(\tau) d\tau}{|\cos(\omega\tau)|} [q(x_{t'}^+, t' - \tau) + q(x_{t'}^-, t' - \tau)]. \quad (5)$$

We express $p(x, t)$ in terms of Hermite polynomials $H_n(x)$ [45]. These are orthogonal to each other over $(-\infty, \infty)$ with weight $\exp(-x^2)$ [46]. We respectively take

$$\{q(x, t), p(x, t)\} = \sum_{n=0}^{\infty} H_n(x) e^{-x^2} \{T_n(t), \tilde{T}_n(t)\}, \quad (6)$$

where the eigenfunctions $T_n(t)$, $\tilde{T}_n(t)$ are determined in [48]. The PDF composed of Eqs. (S5) and (S6) allows us to calculate the stationary PDF and statistical quantities.

Consider now $\hat{T}_m(s)$, $\hat{\tilde{T}}_m(s)$ for odd m . When $m = 1$ from (S5) we deduce that $\hat{T}_1(s) = \mathcal{L}\{\cos(\omega\tau)\phi(\tau)\} \hat{T}_1(s)$, implying $\hat{T}_1(s) = 0$. Analogously, $\hat{\tilde{T}}_1(s) = 0$ from (S6). By induction, for every odd m , $T_m(t) = \tilde{T}_m(t) = 0$. Therefore in (6) only even terms are left, and thus $q(x, t)$

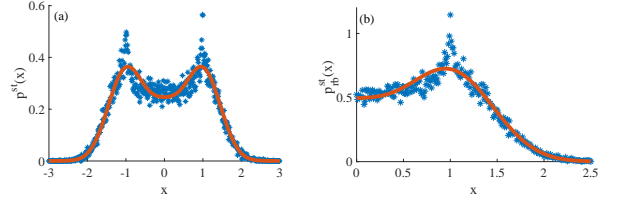


FIG. 1: Stationary PDF of LW in harmonic potential for $\phi(\tau) = \beta e^{-\beta\tau}$, $v_0 = \omega = \beta = 1$. Stars: simulations from 10^4 realizations. (a) No boundaries. Line: approximate theoretical result for $N = 13$ terms and simulation time $t = 10^4$. (b) Reflecting boundary condition at $x = 0$, simulation time $t = 10^3$. Line: approximate result $\lim_{t \rightarrow \infty} \sum_{n=0}^{12} e^{-x^2} H_n \hat{\tilde{T}}_n(t)$.

and $p(x, t)$ are even functions, reflecting the symmetry of the problem. The m th moment is given by $\langle x^m(t) \rangle = i^m \frac{d^m}{dk^m} \bar{p}(k, t) |_{k=0}$, with the Fourier transform $\bar{p}(k, t) = \int_{-\infty}^{\infty} e^{-ikx} p(x, t) dx = \sum_{n=0}^{\infty} \sqrt{\pi} (-ik)^n e^{-k^2/4} \tilde{T}_n(t)$. The Laplace transform of the MSD is $\langle x^2(s) \rangle = \frac{\sqrt{\pi}}{2} \hat{T}_0(s) + 2\sqrt{\pi} \hat{T}_2(s)$, where $\hat{T}_0(s)$ and $\hat{T}_2(s)$ can be obtained from (S6) and (S6). With $\hat{T}_0(s) = (\sqrt{\pi}s)^{-1}$, we have the normalization $\int_{-\infty}^{\infty} p(x, t) dx = \bar{p}(k=0, t) = \sqrt{\pi} \hat{T}_0(t) = 1$.

For the MSD we obtain $\hat{T}_2(s)$, $\hat{\tilde{T}}_2(s)$ from (S5), (S6) for specific $\phi(\tau)$. For the exponential $\phi(\tau) = \beta e^{-\beta\tau}$, we get $\hat{\tilde{T}}_2(s) = \frac{2v_0^2 - \omega^2}{4\sqrt{\pi}\omega^2 s}$. At long t (small s) the asymptotic behavior of the MSD is given by the constant

$$\langle x^2(t) \rangle \sim v_0^2 / \omega^2. \quad (7)$$

For uniform $\phi(\tau) = \frac{1}{T} \mathbf{1}_{[0, T]}(\tau)$ on $[0, T]$ with period $T = 2\pi/\omega$ ($\mathbf{1}_{[0, T]}(\tau)$ is the indicator function) as well as for the asymptotic power-law $\phi(\tau) = \alpha/(1+\tau)^{1+\alpha}$ ($\alpha > 0$) we find the same plateau (7). Thus LWs in a harmonic potential always localize asymptotically and the plateau value only depends on the stiffness of the potential as well as the speed v_0 and mass of the particle. The form of $\phi(\tau)$ has no influence on the plateau (7) and the sufficiently fast decay of $p^{\text{st}}(x)$ at $|x| \rightarrow \infty$ (see also below).

The stationary PDF follows from the final value theorem of the Laplace transform, $p^{\text{st}}(x) = \lim_{t \rightarrow \infty} p(x, t) = \lim_{s \rightarrow 0} s \hat{p}(x, s) = \lim_{s \rightarrow 0} \sum_{n=0}^{\infty} H_{2n}(x) e^{-x^2} s \hat{\tilde{T}}_{2n}(s)$, and $\hat{\tilde{T}}_{2n}(s)$ is given by (S5), (S6). For explicit calculations we truncate the series after N terms, to obtain the approximate stationary PDF for sufficiently large N . We choose $\phi(\tau) = e^{-\tau}$ and $v_0/\omega = 1$. For $N = 13$ we find the approximate stationary PDF in [48], as shown in Fig. 1a. Despite the potential minimum at the origin, $p^{\text{st}}(x)$ is distinctly bimodal with maximum at $|x| \approx v_0/\omega$. Physically, the peaks emerge due to the fact that each jump starting at the origin actually points away from $x = 0$. We would thus expect that for sufficiently large v_0 and appropriate systems parameters the bimodality occurs. Note that similar effects are indeed known from LFs: an LF in a harmonic potential is stationary and monomodal

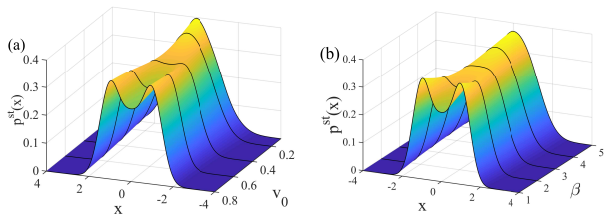


FIG. 2: Stationary PDF [48] for $\phi(\tau) = \beta e^{-\beta\tau}$ with $\beta = 1$ and varying v_0 , and $v_0 = 1$ and changing β with $v_0/\omega = 1$ fixed. In both cases a monomodal-to-bimodal crossover occurs.

[20], yet in steeper than harmonic potentials LF's are bimodal [23]. We now further explore $p^{\text{st}}(x)$.

As shown in Fig. 2 for exponential $\phi(\tau)$ [48] the bimodality of $p^{\text{st}}(x)$ indeed depends on the exact parameters. Once v_0 is small or β becomes large, i.e., when the LW approaches the limit of a regular random walk, monomodality is restored. As shown in Fig. S1 similar behaviors occur for uniform and power-law forms of $\phi(\tau)$. The crossover can in fact be quite delicate; see Fig. S1.

The tails of the stationary PDF are characterized by the kurtosis $K = \langle x^4(t) \rangle / \langle x^2(t) \rangle^2$. When $\phi(\tau) = \beta e^{-\beta\tau}$, Eqs. (S5) and (S6) lead to $\langle \hat{x}^4(s) \rangle = 3\sqrt{\pi}\hat{T}_0/4 + 6\sqrt{\pi}\hat{T}_2 + 24\sqrt{\pi}\hat{T}_4 \sim [3v_0^4(\beta^2 + 6\omega^2)] / [\omega^2(\beta^2 + 10\omega^2)]$, i.e.

$$K = [3(\lambda^2 + 6\omega^2)] / (\lambda^2 + 10\omega^2). \quad (8)$$

This form is verified by simulations in Fig. 3a. We note that, in contrast to the MSD, the kurtosis depends on the shape of $\phi(\tau)$. For small inverse time scales β , the K values show that the PDF is platykurtic and converges to the Gaussian value $K = 3$ for large β . In this limit we expect the LW to converge to a normal random walk, for which the PDF is Gaussian in a harmonic potential. Analogous behavior is found for uniform $\phi(\tau) = \mathbf{1}_{[0, 2\pi r/\omega]}(\tau)$ [48], Fig. 3b. For small interval r , a Gaussian emerges, as $K \sim 3 - 2.4\pi^2 r^2$. For an asymptotic power-law form $\phi(\tau) = \alpha/(1 + \tau)^{1+\alpha}$ simulations show that K assumes platykurtic values even for $\alpha > 2$ (Fig. 3c).

Relaxation dynamics. We now discuss the relaxation of the LW particle in the harmonic potential with initial position $x_0 \neq 0$, i.e., $p_0(x) = \delta(x - x_0)$ for different forms of the waiting time $\phi(\tau)$. The mean position is obtained as $\langle x(t) \rangle = \sqrt{\pi}\tilde{T}_1(t)$, where $\tilde{T}_1(t)$ is given through

$$\hat{\tilde{T}}_1(s) = \frac{x_0 \mathcal{L}\{\cos(\omega\tau)\Psi(\tau)\}}{\sqrt{\pi}(1 - \mathcal{L}\{\cos(\omega\tau)\phi(\tau)\})}. \quad (9)$$

With $\mathcal{L}\{\cos(\omega t)f(t)\} = \frac{1}{2}(\hat{f}(s + i\omega) + \hat{f}(s - i\omega))$ we get

$$\hat{\tilde{T}}_1(s) = \frac{x_0}{\sqrt{\pi}} \frac{\frac{1 - \hat{\phi}(s - i\omega)}{s - i\omega} + \frac{1 - \hat{\phi}(s + i\omega)}{s + i\omega}}{2 - \hat{\phi}(s - i\omega) - \hat{\phi}(s + i\omega)}. \quad (10)$$

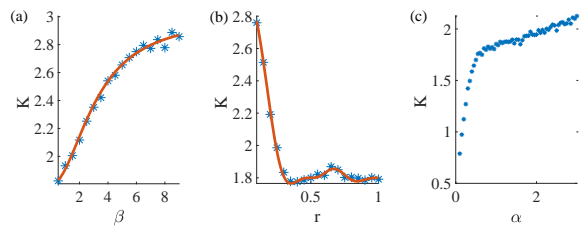


FIG. 3: Stationary value of the kurtosis K for three $\phi(\tau)$ for $v_0 = \omega = 1$, averaged over 5×10^4 trajectories and simulation time $t = 10^4$: (a) $\phi(\tau) = \beta e^{-\beta\tau}$ as function of β ; (b) $\phi(\tau) = \mathbf{1}_{[0, 2\pi r/\omega]}(\tau)$ versus r ; (c) $\phi(\tau) = \alpha/(1 + \tau)^{1+\alpha}$ versus α . Values below 3 indicate that the PDF is platykurtic.

For an exponential $\phi(\tau)$ we find $\langle \hat{x}(s) \rangle = \frac{x_0(s + \beta)}{s^2 + \omega^2 + \beta s}$, i.e.,

$$\begin{aligned} \langle x(t) \rangle &= x_0 \exp(-[\beta + \sqrt{\beta^2 - 4\omega^2}]t/2) \\ &\times \frac{1}{2} \left[\frac{(e^{\sqrt{\beta^2 - 4\omega^2}t} - 1)}{\sqrt{1 - 4\omega^2/\beta^2}} \right. \\ &\left. + (e^{\sqrt{\beta^2 - 4\omega^2}t} + 1) \right]; \end{aligned} \quad (11)$$

see Fig. 4a. Thus, the relaxation of the initial position is exponential to leading order. For uniform $\phi(\tau)$ on $[0, T]$ with Laplace transform $\hat{\phi}(s) = (1 - e^{-Ts})/(Ts)$,

$$\begin{aligned} \langle \hat{x}(s) \rangle &= \left[e^{sT}(-s^2 + s^3T + \omega^2 + sT\omega^2) + (s^2 - \omega^2) \right. \\ &\times \cos(\omega T) - 2s\omega \sin(\omega T) \left. \right] / \left[(s^2 + \omega^2) \right. \\ &\left. \times (e^{sT}(-s + s^2T + T\omega^2) + s \cos(\omega T) - \omega \sin(\omega T)) \right], \end{aligned} \quad (12)$$

which we analyze numerically in Fig. 4b. The case of a power-law form for $\phi(\tau)$ can only be solved numerically, after plugging the asymptotic form $\hat{\phi}(s) \sim 1 - s^{-\alpha}$ into (10). The resulting behavior is shown in Fig. 4c.

In Fig. 4 we note the difference in the initial decay rate and the final approach to zero. Curves with higher initial decay appear to converge more slowly due to the apparent oscillations. Their existence reminds inertia effects known from classical oscillators. In the present model they are likely to the initial non-equilibrated speed v_0 for each jump. However, the exact value of v_0 has no influence on the average displacement as seen from (10).

Reflecting boundary condition at $x = 0$. We now consider LWs in a harmonic potential with a reflecting boundary at $x = 0$. On the random walk level when the i th step begins at time t_{i-1} at position $|x_{t_{i-1}}|$, and it then moves to x_{t_i} which may be negative. Then for the $(i + 1)$ th step we take the absolute value of the end displacement of step i , $|x_{t_i}|$, to be the starting position of step $i + 1$. For the last step (n , such that $t_n + \tau > t$), we also need the absolute value $|x_t|$ as the end point of the walk. In order to solve this problem, we first construct an auxiliary process, whose last step is x_t instead of $|x_t|$.

The detailed derivations are found in [48]. Fig. 1b shows the reflected stationary PDF. Note that for the reflected process the PDF $p_{\text{rb}}(|x|, t)$ can be given through

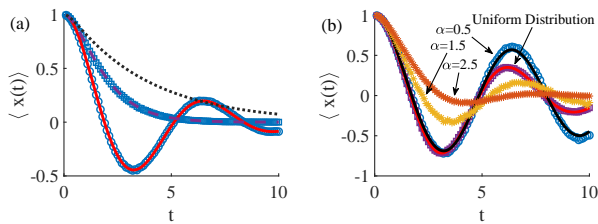


FIG. 4: Simulations results of the relaxation dynamics of the first moment $\langle x(t) \rangle$ from 10^4 realizations each, for $v_0 = \omega = x_0 = 1$. (a) exponential waiting time PDF $\phi(\tau) = \beta e^{-\beta}$ with $\beta = 0.5$ (circles) and $\beta = 2$ (squares). The full, dashed, and dotted (with $\beta = 4$) lines represent the theoretical results. (b) power-law and uniform densities on $[0, 2\pi]$, the lines are from numerical Laplace inversion. Note the oscillatory behavior.

$p_{\text{rb}}(|x|, t) = p_{\text{aux}}(|x|, t) + p_{\text{aux}}(-|x|, t)$. The MSD is $\int_0^\infty x^2 p_{\text{rb}}(x, t) dx = \int_{-\infty}^\infty x^2 p_{\text{aux}}(x, t) dx$, which indicates that the reflected and auxiliary processes have the same MSD, as expected from the applicable method of images. Consequently the asymptotic value of the MSD is given by (7). We note that the horizontal shape of the PDF next to the reflecting boundary is a consequence of the renewal character of the CTRW process. For positively (negatively) correlated stochastic processes an accretion or depletion of probability occurs at the boundary [49].

Conclusions. We considered LWs in a generic external harmonic potential. Apart from being experimentally relevant, our results answer the conceptual question whether and how LWs equilibrate in soft confinement. Our analysis shows that LWs under harmonic confinement equilibrate to a stationary PDF, that, surprisingly, may be bimodal with peak locations $x = \pm v_0/\omega$. However, the bimodality delicately depends on the model parameters. When the LW approaches a regular random walk, monomodality is restored. For exponential and uniform $\phi(\tau)$ we also demonstrated that the stationary PDF in these limits becomes Gaussian. While the stationary

value of the MSD is independent of the chosen form of $\phi(\tau)$ and thus in all cases the tails of the stationary PDF always decay sufficiently fast, higher order moments depend on $\phi(\tau)$. This was discussed for the fourth-order moment entering the kurtosis K . Our results for K show that the stationary PDF is always platykurtic.

The bimodality of LWs in a harmonic external potential are similar to the known results for spatiotemporally decoupled LFs. While LFs are monomodal in a harmonic potential and have diverging MSD, in steeper-than-harmonic potentials LFs assume bimodal stationary PDFs. The main difference is that the stationary PDF of LFs always have a power-law asymptote and thus the kurtosis is either undefined or has a leptokurtic value.

The relaxation dynamics, as discussed for the mean particle position, was studied by analytics and numerics for the three scenarios of the waiting time density $\phi(\tau)$. In particular, we observe characteristic, pseudo-inertial oscillations reflecting the “skater” formulation of the LW process adopted here, namely, that each step starts with a fixed initial speed v_0 . The results are analogous for the case of a reflecting boundary at the origin, for which we showed that the PDF is horizontal at the boundary, in contrast to correlated processes.

Following recent results for the onset of superdiffusion in LWs and their behavior in finite domains [50] our work fills another gap in the description of these widely used spatiotemporally coupled random walks.

Acknowledgments

This work was supported by the National Natural Science Foundation of China, grant 11671182. RM acknowledges the German Science Foundation (DFG), grant ME 1535/7-1 and the Foundation for Polish Science (FNP) for a Humboldt Polish Honorary Research Scholarship.

-
- [1] J.-P. Bouchaud and A. Georges, Phys. Rep. **195**, 127 (1990).
- [2] R. Metzler, J.-H. Jeon, A. G. Cherstvy and E. Barkai, Phys. Chem. Chem. Phys. **16**, 24128 (2014).
- [3] F. Höfling and T. Franosch, Rep. Progr. Phys. **76**, 046602 (2013); K. Nørregaard, R. Metzler, C. Ritter, K. Berg-Sørensen, and L. Oddershede, Chem. Rev. **117**, 4342 (2017).
- [4] H. Scher and E. W. Montroll, Phys. Rev. B **12**, 2455 (1975).
- [5] J. Szymanski and M. Weiss, Phys. Rev. Lett. **103**, 038102 (2009); W. Pan, L. Filobelo, N. D. Q. Pham, O. Galkin, V. V. Uzunova, and P. G. Vekilov Phys. Rev. Lett. **102**, 058101 (2009); J.-H. Jeon, N. Leijnse, L. B. Oddershede, and R. Metzler, New J. Phys. **15**, 045011 (2013).
- [6] P. Schuille, U. Haupts, S. Maiti, and W. W. Webb, Biophys. J. **77**, 2251 (1999); M. Weiss, H. Hashimoto, and T. Nilsson, Biophys. J. **84**, 4043 (2003); S. Gupta, J. U. de Mel, R. M. Perera, P. Zolnierczuk, M. Bleuel, A. Faraone, and G. J. Schneider, J. Phys. Chem. Lett. **9**, 2956 (2018); W. He, H. Song, Y. Su, L. Geng, B. J. Ackerson, H. B. Peng, and P. Tong, Nat. Comm. **7**, 11701 (2016).
- [7] A. V. Weigel, B. Simon, M. M. Tamkun and D. Krapf, Proc. Natl. Acad. Sci. U. S. A. **108**, 6438 (2011); C. Manzo, J. A. Torreno-Pina, P. Massignan, G. J. Lapeyre, Jr., M. Lewenstein, and M. F. Garcia Parajo, Phys. Rev. X **5**, 011021 (2015).
- [8] G. R. Kneller, K. Baczynski, and M. Pasienkewicz-Gierula, J. Chem. Phys. **135**, 141105 (2011); J.-H. Jeon, H. M. Monne, M. Javanainen, and R. Metzler, Phys. Rev. Lett. **109**, 188103 (2012); J.-H. Jeon, M. Javanainen, H. Martinez-Seara, R. Metzler, and I. Vattulainen, Phys. Rev. X **6**, 021006 (2016).
- [9] S. C. Weber, A. J. Spakowitz, and J. A. Theriot, Phys.

- Rev. Lett. **104**, 238102 (2010); I. Golding and E. C. Cox, Phys. Rev. Lett. **96**, 098102 (2006); I. Bronstein, Y. Israel, E. Kepten, S. Mai, Y. Shav-Tal, E. Barkai and Y. Garini, Phys. Rev. Lett. **103**, 018102 (2009); J.-H. Jeon, V. Tejedor, S. Burov, E. Barkai, C. Selhuber-Unkel, K. Berg-Sørensen, L. Oddershede, and R. Metzler, Phys. Rev. Lett. **106**, 048103 (2011).
- [10] S. M. Tabei, S. Burov, H. Y. Kim, A. Kuznetsov, T. Huynh, J. Jureller, L. H. Philipson, A. R. Dinner, and N. F. Scherer, Proc. Natl. Acad. Sci. U.S.A. **110**, 4911 (2013).
- [11] Y. Edery, H. Scher, A. Guadagnini, and B. Berkowitz, Water Res. Res. **50**, 1490 (2014); N. Goepfert, N. Goldscheider, and B. Berkowitz, Water Res. Res., in press, DOI:10.1016/j.watres.2020.115755.
- [12] D. Robert, T. H. Nguyen, F. Gallet, and C. Wilhelm, PLoS ONE **4**, e10046 (2010); A. Caspi, R. Granek, and M. Elbaum. Phys. Rev. Lett. **85**, 5655 (2000).
- [13] J. F. Reverey, J.-H. Jeon, M. Leippe, R. Metzler, and C. Selhuber-Unkel, Sci. Rep. **5**, 11690 (2015).
- [14] G. Seisenberger, M. U. Ried, T. Endreß, H. Büning, M. Hallek, and C. Bräuchle, Science **294**, 1929 (2001).
- [15] G. Boffetta and I. M. Sokolov, Phys. Rev. Lett. **88**, 094501 (2002).
- [16] E. W. Montroll and G. H. Weiss, J. Math. Phys. **10**, 753 (1969).
- [17] R. Metzler and J. Klafter, Phys. Rep. **339**, 1 (2000).
- [18] R. Metzler, E. Barkai, and J. Klafter, Phys. Rev. Lett. **82**, 3563 (1999); Europhys. Lett. **46**, 431 (1999).
- [19] H. C. Fogedby, Phys. Rev. E **50**, 1657 (1994); *ibid.* **58**, 1690 (1998); Phys. Rev. Lett. **73**, 2517 (1994).
- [20] S. Jespersen, R. Metzler, and H. C. Fogedby, Phys. Rev. E **59** 2736 (1999).
- [21] G.M. Viswanathan, V. Afanasyev, S.V. Buldyrev, E.J. Murphy, P.A. Prince, and H.E. Stanley, Nature **381**, 413 (1996); G. M Viswanathan, M. G. E. da Luz, E. P. Raposo, and H. E. Stanley, The Physics of Foraging (Cambridge University Press, Cambridge, 2011).
- [22] V. V. Palyulin, A. V. Chechkin, and R. Metzler, Proc. Natl. Acad. Sci. USA **111**, 2931 (2014).
- [23] A. V. Chechkin, J. Klafter, V. Yu. Gonchar, R. Metzler, and L. V. Tanatarov, Phys. Rev. E **67**, 010102(R) (2003); A. V. Chechkin, V. Yu. Gonchar, J. Klafter, and R. Metzler, Phys. Rev. E **72** 010101(R) (2005).
- [24] M. F. Shlesinger, J. Klafter and Y. M. Wong, J. Stat. Phys. **27**, 499 (1982); M. F. Shlesinger and J. Klafter, Phys. Rev. Lett. **54**, 2551 (1985).
- [25] V. Zaburdaev, S. Denisov, and J. Klafter, Rev. Mod. Phys. **87**, 483 (2015).
- [26] P. Cipriani, S. Denisov, and A. Politi, Phys. Rev. Lett. **94**, 244301 (2005); A. Dhar, K. Saito, B. Derrida, Phys. Rev. E **87**, 010103(R) (2013).
- [27] E. Barkai, V. Fleurov, and J. Klafter, Phys. Rev. E **61**, 1164 (2000).
- [28] R. Patel and R. Mehta, J. Nanophot. **6**, 069503 (2012); P. Barthelemy, J. Bertolotti, and D. S. Wiersma, Nature **453**, 495 (2008).
- [29] M. A. Lomholt, T. Koren, R. Metzler, and J. Klafter, Proc. Natl. Acad. Sci. USA **105**, 11055 (2008).
- [30] D. W. Sims, N. E. Humphries, N. Hu, V. Medan, and J. Berni, eLife **8**, e50316 (2019).
- [31] V. V. Palyulin, G. Blackburn, M. A. Lomholt, N. Watkins, R. Metzler, R. Klages, and A. V. Chechkin, New J. Phys. **21**, 103028 (2019).
- [32] M. S. Abe, E-print bioRxiv:2020.01.27.920801.
- [33] M. S. Song, H. C. Moon, J.-H. Jeonm, and H. Y. Park, Nature Comm. **9**, 344 (2018); K. J. Chen, B. Wang, and S. Granick, Nature Mater. **14**, 589 (2015).
- [34] S. Huda et al., Nature Comm. **9**, 4539 (2018).
- [35] D. A. Raichlen, B. M. Wood, A. D. Gordon, A. Z. Mabulla, F. W. Marlowe, and H. Pontzer, Proc. Natl. Acad. Sci. USA **111**, 728 (2014).
- [36] H. Murakami, C. Feliciani, and K. Nishinari, J. Roy. Soc. Interface **16**, 20180939 (2019).
- [37] V. Fioriti, F. Fratichini, S. Chiesa, and C. Moriconi, Int. J. Adv. Robot. Syst. **12**, 98 (2015); Y. Katada, A. Nishiguchi, K. Moriwaki, and R. Qatakabe, Artif. Life Robot. **21**, 295 (2016).
- [38] D. Brockmann, L. Hufnagel, and T. Geisel, Nature **439**, 462 (2006); A. Reynolds, E. Ceccon, C. Baldauf, T. K. Medeiros, and O. Miramontes, PLoS ONE **13**, e0199099 (2018).
- [39] B. Gross, Z. Zheng, S. Liu, X. Chen, A. Sela, J. Li, D. Li, and S. Havlin, E-print arXiv:2003.08382.
- [40] D. Froemberg and E. Barkai, Phys. Rev. E **87**, 030104(R) (2013); Euro. Phys. J. B **86**, 331 (2013).
- [41] A. Godec and R. Metzler, Phys. Rev. Lett. **110**, 020603 (2013); Phys. Rev. E **88**, 012116 (2013).
- [42] A. Rebenshtok, S. Denisov, P. Hänggi and E. Barkai, Phys. Rev. Lett. **112**, 110601 (2014).
- [43] I. M. Sokolov and R. Metzler, Phys. Rev. E **67**, 010101(R) (2003).
- [44] R. Friedrich, F. Jenko, A. Baule and S. Eule, Phys. Rev. Lett. **96**, 230601 (2006); Phys. Rev. E **74**, 041103 (2006).
- [45] P. B. Xu and W. H. Deng, J. Stat. Phys. **173**, 1598 (2018).
- [46] M. Abramowitz and I. A. Stegun, *Handbook of Mathematical Functions* (Dover, New York, 1972).
- [47] P. B. Xu, W. H. Deng and T. Sandev, J. Phys. A: Math. Theor. **53**(11), 115002 (2020).
- [48] Supplemental material
- [49] A. H. O. Wada and T. Vojta, Phys. Rev. E **97**, 020102(R) (2018); T. Guggenberger, G. Pagnini, T. Vojta, and R. Metzler, New J. Phys **21**, 022002 (2019).
- [50] A. Miron, Phys. Rev. E **100**, 012106 (2019); Phys. Rev. Lett, **124**, 140601 (2020).

Supplementary material: Lévy walk dynamics in an external harmonic potential

I. AUXILIARY CALCULATIONS FOR THE EIGENFUNCTION EXPRESSION OF THE PROBABILITY DENSITY FUNCTION

Starting with expression (6) of the main text we now define $\langle f(ax+b), g(cx+d) \rangle = \int_{-\infty}^{\infty} f(ax+b)g(cx+d)e^{-(ax+b)^2} dx$, which does not satisfy linearity. We insert $q(x, t)$ from Eq. (6) into Eq. (3), multiply by $H_m(x)$ ($m = 0, 1, \dots$) on both sides, and integrate x over $(-\infty, \infty)$:

$$\begin{aligned}
& \sum_{n=0}^{\infty} \langle H_n(x), H_m(x) \rangle T_n(t) - H_m(0)\delta(t) \\
&= \frac{1}{2} \sum_{n=0}^{\infty} \int_0^t d\tau \left[\langle H_n\left(\frac{x}{\cos(\omega\tau)} + \frac{v_0}{\omega} \tan(\omega\tau)\right), H_m(x) \rangle \right. \\
&+ \left. \langle H_n\left(\frac{x}{\cos(\omega\tau)} - \frac{v_0}{\omega} \tan(\omega\tau)\right), H_m(x) \rangle \right] \frac{\phi(\tau)T_n(t-\tau)}{|\cos(\omega\tau)|} \\
&= \frac{1}{2} \sum_{n=0}^{\infty} \int_0^t d\tau \left[\langle H_n(y), H_m\left(\cos(\omega\tau)y - \frac{v_0}{\omega} \sin(\omega\tau)\right) \rangle \right. \\
&+ \left. \langle H_n(y), H_m\left(\cos(\omega\tau)y + \frac{v_0}{\omega} \sin(\omega\tau)\right) \rangle \right] \phi(\tau)T_n(t-\tau).
\end{aligned} \tag{S13}$$

We invoke the properties of the Hermite polynomials [1, 2]

$$\langle H_m(x), H_n(x) \rangle = 2^n n! \sqrt{\pi} \delta_{n,m} \tag{S14}$$

with the Kronecker $\delta_{n,m}$, and

$$H_n(x+y) = \sum_{k=0}^n \binom{n}{k} H_k(x) (2y)^{n-k}, \tag{S15}$$

$$H_n(\gamma x) = \sum_{i=0}^{\lfloor \frac{n}{2} \rfloor} \gamma^{n-2i} (\gamma^2 - 1)^i \binom{n}{2i} \frac{2i!}{i!} H_{n-2i}(x), \tag{S16}$$

where $\lfloor \frac{n}{2} \rfloor$ is the biggest integer smaller than $\frac{n}{2}$. Laplace transforming, $\hat{f}(s) = \mathcal{L}\{f(t)\} = \int_0^{\infty} e^{-st} f(t) dt$ yields

$$\begin{aligned}
& \hat{T}_m(s) - \frac{H_m(0)}{\sqrt{\pi} 2^m m!} \\
&= \sum_{k=0}^m \sum_{i=0}^{\lfloor \frac{k}{2} \rfloor} \frac{2^{-2i-1}}{(m-k)! i!} \left(\frac{v_0}{\omega}\right)^{m-k} [(-1)^i + (-1)^{m-k+i}] \\
&\times \mathcal{L}\{\sin^{m-k+2i}(\omega\tau) \cos^{k-2i}(\omega\tau) \phi(\tau)\} \hat{T}_{k-2i}(s).
\end{aligned} \tag{S17}$$

Similarly, we obtain the corresponding relation

$$\begin{aligned}
& \hat{\hat{T}}_m(s) = \sum_{k=0}^m \sum_{i=0}^{\lfloor \frac{k}{2} \rfloor} \frac{(-1)^i 2^{-2i-1}}{(m-k)! i!} \left(\frac{v_0}{\omega}\right)^{m-k} [1 + (-1)^{m-k}] \\
&\times \mathcal{L}\{\cos^{k-2i}(\omega\tau) \sin^{m-k+2i}(\omega\tau) \Psi(\tau)\} \hat{\hat{T}}_{k-2i}(s).
\end{aligned} \tag{S18}$$

Eqs. (S17) and (S18) are used in the main text.

II. NUMERICAL SIMULATIONS OF STATIONARY PDF

Supplementing the behavior of the stationary LW-PDF $p^{\text{st}}(x)$ for exponential waiting time density shown in the main text, we here present analogous results for other forms of $\phi(\tau)$ and variations of the associated parameters.

First for the asymptotic power-law form $\phi(\tau) = \alpha/(1+\tau)^{1+\alpha}$, Fig. S1a and S1b show the effect of different speed v_0 at the beginning of each jump, and of different powers α . As we can see, when v_0 and ω are sufficiently large, a bimodal stationary state emerges. Similarly, when α is below the value 2 and thus the density $\phi(\tau)$ abides to sufficiently long tails, bimodality is observed. Note that the numerical accuracy we can achieve is not sufficient to numerically pin down the crossover to monomodal behavior at exactly $\alpha = 2$, but from the mathematical nature of power-law distributions this assumption appears consequent. Second, we consider the uniform density $\phi(\tau) = \mathbf{1}_{[0, 2\pi r/\omega]}(\tau)$ in Fig. S1c and d for different interval lengths r and ω . When each of the two parameters becomes sufficiently small, monomodality is restored. Note the delicate variation of the shapes with the second digit of these parameters.

III. CALCULATION OF $\langle x^4(t) \rangle$ FOR LW IN HARMONIC POTENTIAL

In the main text we provided the kurtosis for the case of an exponential waiting time density $\phi(\tau)$. For the asymptotic power-law form for $\phi(\tau)$ we resort to simulations. Here we calculate the fourth-order moment and the kurtosis of an LW in a harmonic potential and without boundaries for the case of uniformly distributed waiting time density $\phi(\tau)$ defined on $[0, 2\pi r/\omega]$, $r > 0$. For this case, considering Eqs. (S17) and (S18), the following results can be obtained,

$$\begin{aligned} \lim_{t \rightarrow \infty} T_0(t) &= \frac{\omega}{\pi^{3/2}r}; \\ \lim_{t \rightarrow \infty} \tilde{T}_0(t) &= \frac{1}{\sqrt{\pi}}; \\ \lim_{t \rightarrow \infty} T_2(t) &= \frac{2v_0^2 - \omega^2}{4\pi^{3/2}r\omega}; \\ \lim_{t \rightarrow \infty} \tilde{T}_2(t) &= \frac{2v_0^2 - \omega^2}{4\sqrt{\pi}\omega^2}; \\ \lim_{t \rightarrow \infty} T_4(t) &= \frac{24\pi r(12v_0^4 - 20v_0^2\omega^2 + 5\omega^4) - 8(4v_0^4 - 12v_0^2\omega^2 + 3\omega^4)\sin(4\pi r) + (-20v_0^4 + 12v_0^2\omega^2 - 3\omega^4)\sin(8\pi r)}{96\pi^{3/2}r\omega^3(40\pi r - 8\sin(4\pi r) - \sin(8\pi r))}; \\ \lim_{t \rightarrow \infty} \tilde{T}_4(t) &= [24\pi r v_0^4 + 1152\pi^3 r^3 v_0^4 - 1920\pi^3 r^3 v_0^2 \omega^2 + 480\pi^3 r^3 \omega^4 - 32\pi r v_0^4 \cos(4\pi r) + 8\pi r v_0^4 \cos(8\pi r) + 5v_0^4 \sin(4\pi r) \\ &\quad - 192\pi^2 r^2 v_0^4 \sin(4\pi r) + 384\pi^2 r^2 v_0^2 \omega^2 \sin(4\pi r) - 96\pi^2 r^2 \omega^4 \sin(4\pi r) - 4v_0^4 \sin(8\pi r) - 48\pi^2 r^2 v_0^4 \sin(8\pi r) \\ &\quad + 48\pi^2 r^2 v_0^2 \omega^2 \sin(8\pi r) - 12\pi^2 r^2 \omega^4 \sin(8\pi r) + v_0^4 \sin(12\pi r)] / [384\pi^{5/2} r^2 \omega^4 (40\pi r - 8\sin(4\pi r) - \sin(8\pi r))]. \end{aligned}$$

Therefore,

$$\begin{aligned} \lim_{t \rightarrow \infty} \langle x^4(t) \rangle &= \frac{3\sqrt{\pi}}{4} \lim_{t \rightarrow \infty} \tilde{T}_0(t) + 6\sqrt{\pi} \lim_{t \rightarrow \infty} \tilde{T}_2(t) + 24\sqrt{\pi} \lim_{t \rightarrow \infty} \tilde{T}_4(t) \\ &= v_0^4 [24\pi r + 1152\pi^3 r^3 - 32\pi r \cos(4\pi r) + 8\pi r \cos(8\pi r) + 5\sin(4\pi r) - 192\pi^2 r^2 \sin(4\pi r) - 4\sin(8\pi r) \\ &\quad - 48\pi^2 r^2 \sin(8\pi r) + \sin(12\pi r)] / [16\pi^2 r^2 \omega^4 (40\pi r - 8\sin(4\pi r) - \sin(8\pi r))], \\ \lim_{t \rightarrow \infty} K &= [24\pi r + 1152\pi^3 r^3 - 32\pi r \cos(4\pi r) + 8\pi r \cos(8\pi r) + 5\sin(4\pi r) - 192\pi^2 r^2 \sin(4\pi r) - 4\sin(8\pi r) \\ &\quad - 48\pi^2 r^2 \sin(8\pi r) + \sin(12\pi r)] / [16\pi^2 r^2 (40\pi r - 8\sin(4\pi r) - \sin(8\pi r))]. \end{aligned}$$

The series expansion of the kurtosis for small interval sizes r then becomes

$$K \sim 3 - \frac{12}{5}\pi^2 r^2 + \frac{88}{105}\pi^4 r^4 + \dots,$$

quoted in the main text.

IV. SIMPLIFICATION OF THE GOVERNING EQUATION FOR THE PDF OF VELOCITY DIRECTION CHANGE AT A GIVEN POSITION

In the presence of a *reflecting boundary* we introduce the reflecting condition as outlined in the main text. To construct the auxiliary function we proceed as follows. Changing the initial condition of Eq. (1) in the main text from x_{t_i} to $|x_{t_i}|$, we have $x_{t_i} = A \cos(\omega\tau' \pm \varphi_{\pm v_0})$, where $A = \sqrt{x_{t_i}^2 + v_0^2/\omega^2}$ and $\varphi_{\pm v_0} = \arctan(\frac{\mp v_0}{\omega|x_{t_i}|})$. Denoting the

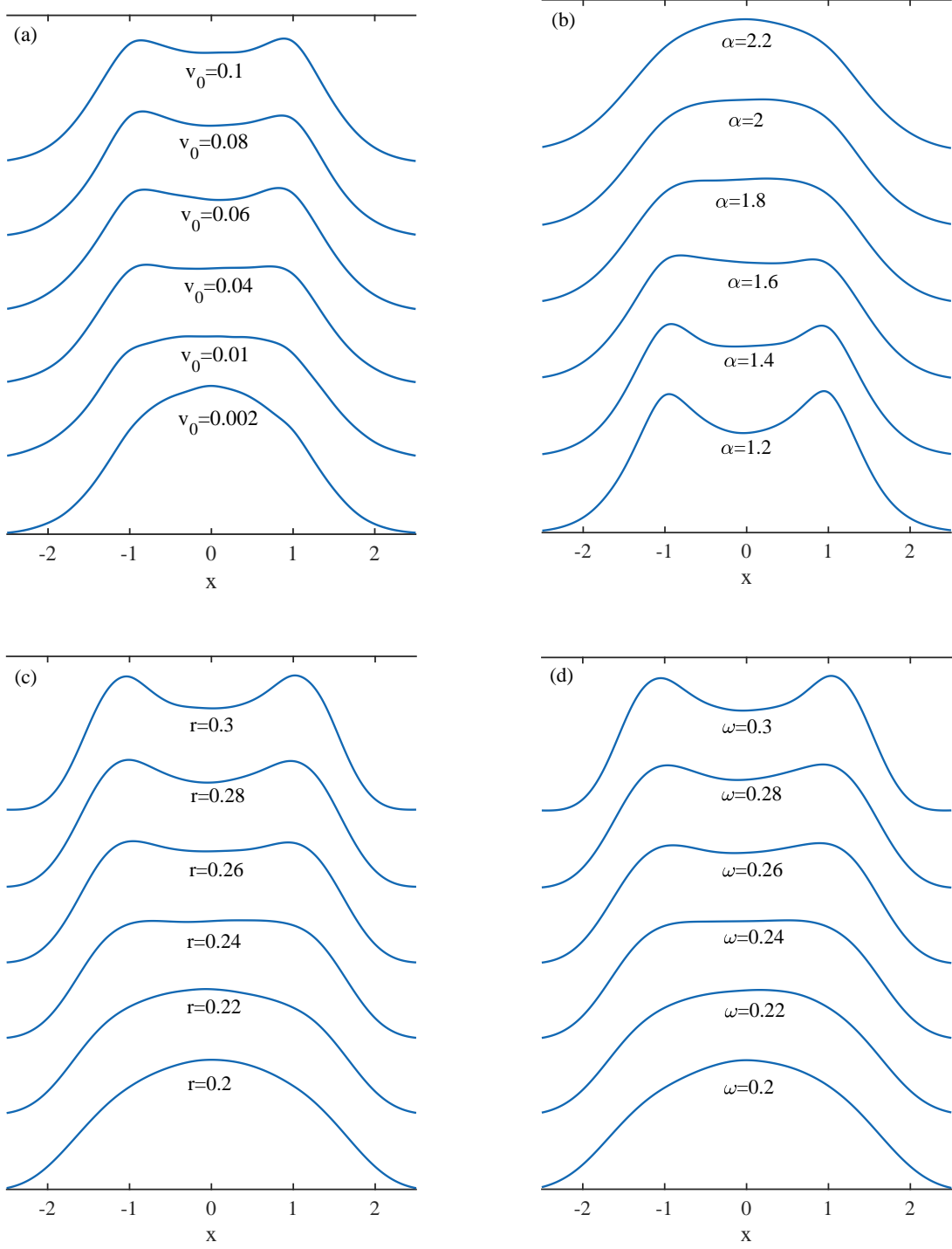


FIG. S1: Stationary PDFs from numerical simulations. For (a) and (b) the asymptotic power-law waiting time PDF $\phi(\tau) = \alpha/(1 + \tau)^{1+\alpha}$ was used with $v_0 = \omega$. For (a) $\alpha = 1.5$ and in (b) $v_0 = 0.1$. For (c) and (d), the uniform waiting time PDF $\phi(\tau) = \mathbf{1}_{[0, 2\pi r/\omega]}(\tau)$ was used with $v_0 = \omega$. In (c) $v_0 = 1$, and for (d) $v_0 = \omega = r$, so that the $\phi(\tau)$ are always the same.

auxiliary process as $q_{\text{aux}}(x_t, t)$, changing velocity direction at position x_t at time t , and taking $p_{\text{aux}}(x, t)$ as the PDF of finding the auxiliary process staying at x at time t . Therefore we have

$$q_{\text{aux}}(x_t, t) = \int_{-\infty}^{\infty} \int_0^t q_{\text{aux}}(x_{t-\tau}, t-\tau) v(x_t, x_{t-\tau}, \tau) \phi(\tau) d\tau dx_{t-\tau} + p_0(x) \delta(t), \quad (\text{S19})$$

where $\delta(\cdot)$ represents the Dirac δ -function, $p_0(x)$ is the initial PDF, $v(x_t, x_{t-\tau}, \tau) = \frac{1}{2} \delta(x_t - A \cos(\omega\tau + \varphi_{v_0})) + \frac{1}{2} \delta(x_t - A \cos(\omega\tau + \varphi_{-v_0}))$, $\varphi_{\pm v_0} = \arctan\left(\frac{\mp v_0}{\omega|x_{t-\tau}|}\right)$ for $x_{t-\tau} \neq 0$, $\varphi_{\pm v_0} = \mp \frac{\pi}{2}$ when $x_{t-\tau} = 0$. According to probability theory, if we choose the initial distribution as $p_0(x) = \delta(x)$, that is $x_{t-\tau} \equiv 0$ when $t-\tau = 0$, and the probability distribution at a given point $t = \tau$ is zero, then the probability of $x_{t-\tau} = 0$ is also zero when $t - \tau \neq 0$. Thus, without loss of generality, in the following we only need to consider $x_{t-\tau} \neq 0$. Moreover, it can be verified that

$$v(x_t, x_{t-\tau}, \tau) = \frac{1}{2} \delta\left(x_t - \sqrt{x_{t-\tau}^2 + \frac{v_0^2}{\omega^2}} \cos\left(\omega\tau + \arctan\left(\frac{-v_0}{\omega x_{t-\tau}}\right)\right)\right) + \frac{1}{2} \delta\left(x_t - \sqrt{x_{t-\tau}^2 + \frac{v_0^2}{\omega^2}} \cos\left(\omega\tau + \arctan\left(\frac{v_0}{\omega x_{t-\tau}}\right)\right)\right). \quad (\text{S20})$$

Consider the property of the δ -function

$$\delta(g(x)) = \sum_i \frac{\delta(x - x_i)}{|g'(x_i)|}, \quad (\text{S21})$$

where x_i is the root of $g(x) = 0$ and the sum in Eq. (S21) extends over all roots. In order to utilize Eq. (S21) to simplify $v(x, \tau)$, we need to solve the following equations first

$$x_t - \sqrt{x_{t-\tau}^2 + \frac{v_0^2}{\omega^2}} \cos\left(\omega\tau + \arctan\left(\frac{-v_0}{\omega x_{t-\tau}}\right)\right) = 0, \quad (\text{S22})$$

$$x_t - \sqrt{x_{t-\tau}^2 + \frac{v_0^2}{\omega^2}} \cos\left(\omega\tau + \arctan\left(\frac{v_0}{\omega x_{t-\tau}}\right)\right) = 0. \quad (\text{S23})$$

From Eq. (S22), there exists

$$x_t = \frac{\sqrt{\omega^2 x_{t-\tau}^2 + v_0^2}}{\omega} \left[\cos(\omega\tau) \frac{\omega|x_{t-\tau}|}{\sqrt{\omega^2 x_{t-\tau}^2 + v_0^2}} + \sin(\omega\tau) \frac{v_0|x_{t-\tau}|}{x_{t-\tau} \sqrt{\omega^2 x_{t-\tau}^2 + v_0^2}} \right],$$

which can be equivalently written as

$$x_{t-\tau} = \begin{cases} \frac{x_t}{\cos(\omega\tau)} - \frac{v_0}{\omega} \tan(\omega\tau), & \text{if } x_{t-\tau} > 0; \\ -\frac{x_t}{\cos(\omega\tau)} - \frac{v_0}{\omega} \tan(\omega\tau), & \text{if } x_{t-\tau} < 0. \end{cases} \quad (\text{S24})$$

Moreover, it can be obtained that $|g'(x_{t-\tau})| = |\cos(\omega\tau)|$, where here $g(y) = x_t - \sqrt{y^2 + \frac{v_0^2}{\omega^2}} \cos\left(\omega\tau + \arctan\left(\frac{-v_0}{\omega y}\right)\right)$. Therefore we have

$$\delta(x_t - A \cos(\omega\tau + \varphi_{v_0})) = \frac{\Theta(x_{t-\tau})}{|\cos(\omega\tau)|} \delta\left(x_{t-\tau} - \frac{x_t}{\cos(\omega\tau)} + \frac{v_0}{\omega} \tan(\omega\tau)\right) + \frac{\Theta(-x_{t-\tau})}{|\cos(\omega\tau)|} \delta\left(x_{t-\tau} + \frac{x_t}{\cos(\omega\tau)} + \frac{v_0}{\omega} \tan(\omega\tau)\right), \quad (\text{S25})$$

where $\Theta(x) = 1$ when $x > 0$, otherwise $\Theta(x) = 0$. Similarly we have

$$\delta(x_t - A \cos(\omega\tau + \varphi_{-v_0})) = \frac{\Theta(x_{t-\tau})}{|\cos(\omega\tau)|} \delta\left(x_{t-\tau} - \frac{x_t}{\cos(\omega\tau)} - \frac{v_0}{\omega} \tan(\omega\tau)\right) + \frac{\Theta(-x_{t-\tau})}{|\cos(\omega\tau)|} \delta\left(x_{t-\tau} + \frac{x_t}{\cos(\omega\tau)} - \frac{v_0}{\omega} \tan(\omega\tau)\right). \quad (\text{S26})$$

Combining the definition of $v(x_t, x_{t-\tau}, \tau)$, Eq. (S25) and Eq. (S26), then Eq. (S19) can be rewritten as

$$\begin{aligned}
q_{\text{aux}}(x_t, t) &= \frac{1}{2} \int_0^t \frac{1}{|\cos(\omega\tau)|} q_{\text{aux}} \left(\frac{x_t}{\cos(\omega\tau)} - \frac{v_0}{\omega} \tan(\omega\tau), t - \tau \right) \Theta \left(\frac{x_t}{\cos(\omega\tau)} - \frac{v_0}{\omega} \tan(\omega\tau) \right) \phi(\tau) d\tau \\
&+ \frac{1}{2} \int_0^t \frac{1}{|\cos(\omega\tau)|} q_{\text{aux}} \left(-\frac{x_t}{\cos(\omega\tau)} - \frac{v_0}{\omega} \tan(\omega\tau), t - \tau \right) \Theta \left(\frac{x_t}{\cos(\omega\tau)} + \frac{v_0}{\omega} \tan(\omega\tau) \right) \phi(\tau) d\tau \\
&+ \frac{1}{2} \int_0^t \frac{1}{|\cos(\omega\tau)|} q_{\text{aux}} \left(\frac{x_t}{\cos(\omega\tau)} + \frac{v_0}{\omega} \tan(\omega\tau), t - \tau \right) \Theta \left(\frac{x_t}{\cos(\omega\tau)} + \frac{v_0}{\omega} \tan(\omega\tau) \right) \phi(\tau) d\tau \\
&+ \frac{1}{2} \int_0^t \frac{1}{|\cos(\omega\tau)|} q_{\text{aux}} \left(-\frac{x_t}{\cos(\omega\tau)} + \frac{v_0}{\omega} \tan(\omega\tau), t - \tau \right) \Theta \left(\frac{x_t}{\cos(\omega\tau)} - \frac{v_0}{\omega} \tan(\omega\tau) \right) \phi(\tau) d\tau + p_0(x) \\
&+ \delta(t).
\end{aligned} \tag{S27}$$

V. DERIVATION OF THE RECURSIVE RELATIONS OF $\{\hat{T}_n(s)\}$ AND $\{\hat{\hat{T}}_n(s)\}$

After obtaining Eq. (S27) and assuming that $q_{\text{aux}}(x, t) = \sum_{n=0}^{\infty} H_n(x) e^{-x^2} T_n(t)$, where $H_n(x)$ are Hermite polynomials [1, 2] and $T_n(t)$ are functions to be determined. Then we find

$$\begin{aligned}
\sum_{n=0}^{\infty} H_n(x) e^{-x^2} T_n(t) &= \frac{1}{2} \int_0^t \frac{1}{|\cos(\omega\tau)|} \sum_{n=0}^{\infty} H_n(x^-) e^{-(x^-)^2} T_n(t - \tau) \Theta(x^-) \phi(\tau) d\tau \\
&+ \frac{1}{2} \int_0^t \frac{1}{|\cos(\omega\tau)|} \sum_{n=0}^{\infty} H_n(-x^+) e^{-(x^+)^2} T_n(t - \tau) \Theta(x^+) \phi(\tau) d\tau \\
&+ \frac{1}{2} \int_0^t \frac{1}{|\cos(\omega\tau)|} \sum_{n=0}^{\infty} H_n(x^+) e^{-(x^+)^2} T_n(t - \tau) \Theta(x^+) \phi(\tau) d\tau \\
&+ \frac{1}{2} \int_0^t \frac{1}{|\cos(\omega\tau)|} \sum_{n=0}^{\infty} H_n(-x^-) e^{-(x^-)^2} T_n(t - \tau) \Theta(x^-) \phi(\tau) d\tau + p_0(x) \delta(t),
\end{aligned} \tag{S28}$$

where $x^{\pm} = \frac{x}{\cos(\omega\tau)} \pm \frac{v_0}{\omega} \tan(\omega\tau)$. Multiplying by $H_m(x)$, $m = 0, 1, \dots$ on both sides of Eq. (S28), integrating over $(-\infty, \infty)$ with respect to x , and changing variables, yield

$$\begin{aligned}
&\sum_{n=0}^{\infty} \int_{-\infty}^{\infty} H_n(x) H_m(x) e^{-x^2} T_n(t) \\
&= \frac{1}{2} \int_0^{\infty} \int_0^t \sum_{n=0}^{\infty} H_n(y) H_m \left(\cos(\omega\tau)y + \frac{v_0}{\omega} \sin(\omega\tau) \right) e^{-y^2} T_n(t - \tau) \phi(\tau) d\tau \\
&+ \frac{1}{2} \int_{-\infty}^0 \int_0^t \sum_{n=0}^{\infty} H_n(y) H_m \left(-\cos(\omega\tau)y - \frac{v_0}{\omega} \sin(\omega\tau) \right) e^{-y^2} T_n(t - \tau) \phi(\tau) d\tau \\
&+ \frac{1}{2} \int_0^{\infty} \int_0^t \sum_{n=0}^{\infty} H_n(y) H_m \left(\cos(\omega\tau)y - \frac{v_0}{\omega} \sin(\omega\tau) \right) e^{-y^2} T_n(t - \tau) \phi(\tau) d\tau \\
&+ \frac{1}{2} \int_{-\infty}^0 \int_0^t \sum_{n=0}^{\infty} H_n(y) H_m \left(-\cos(\omega\tau)y + \frac{v_0}{\omega} \sin(\omega\tau) \right) e^{-y^2} T_n(t - \tau) \phi(\tau) d\tau + H_m(0) \delta(t).
\end{aligned} \tag{S29}$$

First we consider even m . For Hermite polynomials the symmetry relation $H_m(x) = H_m(-x)$ holds for even m , thus the right hand side of Eq. (S29) can be rewritten as

$$\begin{aligned}
&\frac{1}{2} \int_{-\infty}^{\infty} \int_0^t \sum_{n=0}^{\infty} H_n(y) H_m \left(\cos(\omega\tau)y + \frac{v_0}{\omega} \sin(\omega\tau) \right) e^{-y^2} T_n(t - \tau) \phi(\tau) d\tau \\
&+ \frac{1}{2} \int_{-\infty}^{\infty} \int_0^t \sum_{n=0}^{\infty} H_n(y) H_m \left(\cos(\omega\tau)y - \frac{v_0}{\omega} \sin(\omega\tau) \right) e^{-y^2} T_n(t - \tau) \phi(\tau) d\tau + H_m(0) \delta(t).
\end{aligned}$$

With the properties of the Hermite polynomials shown in Eqs. (S15), (S16), we find

$$\begin{aligned} & \sqrt{\pi}2^m m! T_m(t) - (-2)^{\frac{m}{2}} (m-1)!! \delta(t) \\ &= \frac{1}{2} \sum_{j=0}^m \sum_{i=0}^{\lfloor \frac{j}{2} \rfloor} \int_0^t \frac{m! \sqrt{\pi} 2^{j-2i}}{i!(m-j)!} \left(\frac{2v_0}{\omega} \right) [\sin^{m-j}(\omega\tau) + (-\sin(\omega\tau))^{m-k}] \cos^{k-2i}(\omega\tau) (-\sin^2(\omega\tau))^i T_{k-2i}(t-\tau) \phi(\tau) d\tau. \end{aligned}$$

Taking the Laplace transform with respect to t , we finally obtain

$$\begin{aligned} & \sqrt{\pi}2^m m! \hat{T}_m(s) - (-2)^{\frac{m}{2}} (m-1)!! \\ &= \frac{1}{2} \sum_{j=0}^m \sum_{i=0}^{\lfloor \frac{j}{2} \rfloor} \frac{m! \sqrt{\pi} 2^{j-2i}}{i!(m-j)!} \left(\frac{2v_0}{\omega} \right) \mathcal{L} \{ [\sin^{m-j}(\omega\tau) + (-\sin(\omega\tau))^{m-k}] \cos^{k-2i}(\omega\tau) (-\sin^2(\omega\tau))^i \phi(\tau) \} \hat{T}_{k-2i}(s). \end{aligned} \quad (\text{S30})$$

Similarly we assume that $p_{\text{aux}}(x, t) = \sum_{n=0}^{\infty} H_n(x) e^{-x^2} \tilde{T}_n(t)$, and it then follows that

$$\begin{aligned} & \sqrt{\pi}2^m m! \hat{\tilde{T}}_m(s) \\ &= \frac{1}{2} \sum_{j=0}^m \sum_{i=0}^{\lfloor \frac{j}{2} \rfloor} \frac{m! \sqrt{\pi} 2^{j-2i}}{i!(m-j)!} \left(\frac{2v_0}{\omega} \right) \mathcal{L} \{ [\sin^{m-j}(\omega\tau) + (-\sin(\omega\tau))^{m-k}] \cos^{k-2i}(\omega\tau) (-\sin^2(\omega\tau))^i \Psi(\tau) \} \hat{\tilde{T}}_{k-2i}(s), \end{aligned} \quad (\text{S31})$$

where $\Psi(\tau) = \int_{\tau}^{\infty} \phi(\tau') d\tau'$ is the survival probability.

For odd m , the Hermite polynomials satisfy the antisymmetric relation $H_m(x) = -H_m(-x)$, therefore the right hand side of Eq. (S29) can be rewritten as

$$\begin{aligned} & \frac{1}{2} \sum_{n=0}^{\infty} \sum_{j=0}^m \sum_{i=0}^{\lfloor \frac{j}{2} \rfloor} \int_0^t \frac{m!}{i!(j-2i)!(m-j)!} \left[\left(\frac{2v_0}{\omega} \sin(\omega\tau) \right)^{m-j} \cos^{j-2i}(\omega\tau) (-\sin^2(\omega\tau))^i \int_0^{\infty} H_{j-2i}(y) H_n(y) e^{-y^2} dy \right. \\ &+ \left(-\frac{2v_0}{\omega} \sin(\omega\tau) \right)^{m-j} (-\cos(\omega\tau))^{j-2i} (-\sin^2(\omega\tau))^i \int_{-\infty}^0 H_{j-2i}(y) H_n(y) e^{-y^2} dy \\ &+ \left(-\frac{2v_0}{\omega} \sin(\omega\tau) \right)^{m-j} \cos^{j-2i}(\omega\tau) (-\sin^2(\omega\tau))^i \int_0^{\infty} H_{j-2i}(y) H_n(y) e^{-y^2} dy \\ &\left. + \left(\frac{2v_0}{\omega} \sin(\omega\tau) \right)^{m-j} (-\cos(\omega\tau))^{j-2i} (-\sin^2(\omega\tau))^i \int_{-\infty}^0 H_{j-2i}(y) H_n(y) e^{-y^2} dy \right] \phi(\tau) T_n(t-\tau) d\tau, \end{aligned} \quad (\text{S32})$$

which indicates that when m is odd, j in Eq. (S32) must be odd as well, otherwise expression Eq. (S32) equals zero. Therefore Eq. (S32) can be further rewritten as

$$\begin{aligned} & \sum_{n=0}^{\infty} \sum_{j=0}^{\lfloor \frac{m}{2} \rfloor} \sum_{i=0}^j \int_0^t \frac{m!}{i!(2j+1-2i)!(m-2j-1)!} \left(\frac{2v_0}{\omega} \sin(\omega\tau) \right)^{m-2j-1} \cos^{2j+1-2i}(\omega\tau) (-\sin^2(\omega\tau))^i \\ & \left[\int_0^{\infty} H_{2j+1-2i}(y) H_n(y) e^{-y^2} dy - \int_{-\infty}^0 H_{2j+1-2i}(y) H_n(y) e^{-y^2} dy \right] T_n(t-\tau) \phi(\tau) d\tau, \end{aligned} \quad (\text{S33})$$

which indicates that when n is odd, $H_{2j+1-2i}(y) H_n(y) e^{-y^2}$ is an even function, further $\int_0^{\infty} H_{2j+1-2i}(y) H_n(y) e^{-y^2} dy - \int_{-\infty}^0 H_{2j+1-2i}(y) H_n(y) e^{-y^2} dy = 0$, i.e., Eq. (S33) is zero. Therefore, odd terms of $T_n(t)$ disappear and there exists

$$\begin{aligned} \sqrt{\pi}2^m m! T_m(t) &= 2 \sum_{n=0}^{\infty} \sum_{j=0}^{\lfloor \frac{m}{2} \rfloor} \sum_{i=0}^j \frac{m!}{i!(2j+1-2i)!(m-2j-1)!} \int_0^t \left(\frac{2v_0}{\omega} \sin(\omega\tau) \right)^{m-2j-1} \cos^{2j+1-2i}(\omega\tau) (-\sin^2(\omega\tau))^i \\ & \times \int_0^{\infty} H_{2j+1-2i}(y) H_{2n}(y) e^{-y^2} dy T_{2n}(t-\tau) \phi(\tau) d\tau. \end{aligned} \quad (\text{S34})$$

We now use the following property of the Hermite polynomials [3]

$$\int_0^\infty H_{2j+1-2i}(y)H_{2n}(y)e^{-y^2} dy = \frac{\sqrt{\pi} {}_2F_1\left(-2j+1-2i, -2n; 1 - \frac{2j+1-2i}{2} - n; \frac{1}{2}\right)}{2^{1-(2j+1-2i)-2n}\Gamma\left(1 - \frac{2j+1-2i}{2} - n\right)},$$

where ${}_2F_1(a, b; c; d)$ is the hypergeometric function defined as

$${}_2F_1(a, b; c; d) = \sum_{n=0}^{\infty} \frac{(a)_n (b)_n}{(c)_n} \frac{z^n}{n!}.$$

Here $(d)_n$ represents the Pochhammer symbol,

$$(d)_n = \begin{cases} 1, & \text{if } n = 0; \\ d(d+1) \cdots (d+n-1), & \text{if } n > 0. \end{cases}$$

After taking the Laplace transform with respect to t of Eq. (S34) we have

$$\begin{aligned} \sqrt{\pi} 2^m m! \hat{T}_m(s) = & 2 \sum_{n=0}^{\infty} \sum_{j=0}^{\lfloor \frac{m}{2} \rfloor} \sum_{i=0}^j \frac{m! \sqrt{\pi} {}_2F_1\left(-2j+1-2i, -2n; \frac{1}{2} + i - j - n; \frac{1}{2}\right)}{i!(2j+1-2i)!(m-2j-1)!\Gamma\left(\frac{1}{2} + i - j - n\right) 2^{2(i-j-n)}} \left(\frac{2v_0}{\omega}\right)^{m-2j-1} \\ & \times \mathcal{L} \left\{ \sin^{m-2j-1}(\omega\tau) \cos^{2j+1-2i}(\omega\tau) (-\sin^2(\omega\tau))^i \phi(\tau) \right\} \hat{T}_{2n}(s). \end{aligned} \quad (\text{S35})$$

Similarly, for odd m we obtain the relations of $\hat{T}_m(s)$ and $\hat{T}_{2n}(s)$,

$$\begin{aligned} \sqrt{\pi} 2^m m! \hat{T}_m(s) = & 2 \sum_{n=0}^{\infty} \sum_{j=0}^{\lfloor \frac{m}{2} \rfloor} \sum_{i=0}^j \frac{m! \sqrt{\pi} {}_2F_1\left(-2j+1-2i, -2n; \frac{1}{2} + i - j - n; \frac{1}{2}\right)}{i!(2j+1-2i)!(m-2j-1)!\Gamma\left(\frac{1}{2} + i - j - n\right) 2^{2(i-j-n)}} \left(\frac{2v_0}{\omega}\right)^{m-2j-1} \\ & \times \mathcal{L} \left\{ \sin^{m-2j-1}(\omega\tau) \cos^{2j+1-2i}(\omega\tau) (-\sin^2(\omega\tau))^i \Psi(\tau) \right\} \hat{T}_{2n}(s). \end{aligned} \quad (\text{S36})$$

VI. APPROXIMATE STATIONARY DISTRIBUTION FOR LÉVY WALKS IN HARMONIC POTENTIAL WITH FREE AND REFLECTING BOUNDARY CONDITIONS

In this section, we mainly provide the approximate results for the stationary PDF for LWs in a harmonic potential when the duration of individual walk steps τ follows the exponential density $e^{-\tau}$. For simplicity of calculations we take $v_0 = \omega = 1$. First we provide results for free boundary conditions. In this case the odd terms of $\{T_n(t)\}$ and $\{\tilde{T}_n(t)\}$ vanish. Therefore it is sufficient to consider the even terms, which can be represented as the recurrence formulas as Eq. (S17) and Eq. (S18). The behaviors of $\tilde{T}_0(t), \tilde{T}_2(t), \dots, \tilde{T}_{12}(t)$ for $t \rightarrow \infty$ are then

$$\begin{aligned} \lim_{t \rightarrow \infty} \tilde{T}_0(t) &= \frac{1}{\sqrt{\pi}}; \\ \lim_{t \rightarrow \infty} \tilde{T}_2(t) &= \frac{1}{4\sqrt{\pi}}; \\ \lim_{t \rightarrow \infty} \tilde{T}_4(t) &= -\frac{5}{352\sqrt{\pi}}; \\ \lim_{t \rightarrow \infty} \tilde{T}_6(t) &= \frac{63}{2721928\sqrt{\pi}}; \\ \lim_{t \rightarrow \infty} \tilde{T}_8(t) &= \frac{146606719}{5558830238720\sqrt{\pi}}; \\ \lim_{t \rightarrow \infty} \tilde{T}_{10}(t) &= -\frac{39362159928909}{30088502786329292800\sqrt{\pi}}; \\ \lim_{t \rightarrow \infty} \tilde{T}_{12}(t) &= \frac{198428708025937940281}{4895922461868213486986035200\sqrt{\pi}}. \end{aligned}$$

The approximate stationary distribution $p^{\text{st}}(x) \approx \sum_{n=0}^6 \lim_{t \rightarrow \infty} \tilde{T}_{2n}(t) H_{2n}(x) e^{-x^2}$ is shown in Fig. 1 in the main text.

For the case of *reflecting boundary*, the behaviors of $\tilde{T}_0(t), \tilde{T}_2(t), \dots, \tilde{T}_{12}(t)$ are obtained from Eqs. (S30) and (S31) as follows

$$\begin{aligned}\lim_{t \rightarrow \infty} \tilde{T}_0(t) &= \frac{1}{\sqrt{\pi}}; \\ \lim_{t \rightarrow \infty} \tilde{T}_2(t) &= \frac{1}{4\sqrt{\pi}}; \\ \lim_{t \rightarrow \infty} \tilde{T}_4(t) &= -\frac{5}{352\sqrt{\pi}}; \\ \lim_{t \rightarrow \infty} \tilde{T}_6(t) &= -\frac{7}{429440\sqrt{\pi}}; \\ \lim_{t \rightarrow \infty} \tilde{T}_8(t) &= \frac{112707}{4385097728\sqrt{\pi}}; \\ \lim_{t \rightarrow \infty} \tilde{T}_{10}(t) &= -\frac{151918210141}{118676969381273600\sqrt{\pi}}; \\ \lim_{t \rightarrow \infty} \tilde{T}_{12}(t) &= \frac{154859416018475893}{3862161199753787756052480\sqrt{\pi}}.\end{aligned}$$

For the odd terms, due to the involved terms we only use $T_0(t), T_2(t), \dots, T_8(t)$ for their approximate calculations, then utilizing Eq. (S36) leads us to the results

$$\begin{aligned}\lim_{t \rightarrow \infty} \tilde{T}_1(t) &\approx \frac{2124385847}{2740686080\pi}; \\ \lim_{t \rightarrow \infty} \tilde{T}_3(t) &\approx \frac{6463601801}{164441164800\pi}; \\ \lim_{t \rightarrow \infty} \tilde{T}_5(t) &\approx -\frac{18361300219}{3420376227840\pi}; \\ \lim_{t \rightarrow \infty} \tilde{T}_7(t) &\approx -\frac{687695174759}{399043893248000\pi}; \\ \lim_{t \rightarrow \infty} \tilde{T}_9(t) &\approx \frac{70824923727473}{7067865437208576000\pi}; \\ \lim_{t \rightarrow \infty} \tilde{T}_{11}(t) &\approx -\frac{1483140637545367}{1724559166678892544000\pi}.\end{aligned}$$

Finally $p_{\text{aux}}^{\text{st}}(x) \approx \sum_{n=0}^{12} \lim_{t \rightarrow \infty} \tilde{T}_n(t) H_n(x) e^{-x^2}$, showing good convergence for the involved number of terms. The stationary PDF for the case of a reflecting boundary is then $p_{\text{rb}}^{\text{st}}(x) = p_{\text{aux}}^{\text{st}}(x) + p_{\text{aux}}^{\text{st}}(-x)$ for $x \geq 0$. The corresponding simulation results are shown in Fig. 1 of the main text.

[1] M. Abramowitz and I. A. Stegun, *Handbook of Mathematical Functions* (Dover, New York, 1972).

[2] P. B. Xu, W. H. Deng and T. Sandev, *J. Phys. A: Math. Theor.* **53**(11), 115002 (2020).

[3] A. P. Prudnikov, Y. A. Brychkov and O. I. Marichev, *Integral and Series* (Gordon & Breach, New York, 1990).